

Hydrodeoxygenation of Lignin-Derived Phenolic Monomers and Dimers to Alkane Fuels over Bifunctional Zeolite-Supported Metal Catalysts

Wei Zhang,^{†,§} Jinzhu Chen,^{*,†} Ruliang Liu,^{†,§} Shengpei Wang,^{†,§} Limin Chen,[‡] and Kegui Li^{†,§}[†]CAS Key Laboratory of Renewable Energy, Guangzhou Institute of Energy Conversion, Chinese Academy of Sciences, Guangzhou 510640, P. R. China[‡]Guangdong Provincial Key Laboratory of Atmospheric Environment and Pollution Control, College of Environment and Energy, South China University of Technology, Guangzhou 510006, P. R. China[§]University of Chinese Academy of Sciences, Beijing 100049, P. R. China

S Supporting Information

ABSTRACT: A bifunctional catalyst of Ru supported in zeolite HZSM-5, Ru/HZSM-5 (Si/Al = 25), exhibited excellent hydrodeoxygenation activity toward the conversion of lignin-derived phenolic monomers and dimers to cycloalkanes in aqueous solution. The oxygen-containing groups in mono- and binuclear phenols were removed through a cleavage of C–O bonds in phenolics followed by an integrated metal- and acid-catalyzed hydrogenation and dehydration. As a bifunctional catalyst Ru/HZSM-5, the presence of both the Brønsted acid site in the pores of HZSM-5 for dehydration and a metallic function of Ru for hydrogenation was indispensable for the formation of alkanes from lignin-derived phenolics. Our findings also reveal that the Ru/HZSM-5 with the lowest Si/Al ratio of HZSM-5 proved to be most selective to cycloalkanes, indicating that more acid sites over zeolite are favorable for the dehydration of cyclohexanol during hydrodeoxygenation process, which leads higher selectivity to hydrocarbons. This approach for the construction of bifunctional catalyst highlights an efficient route for hydrodeoxygenation of lignin-derived phenolic oil to transportation biofuels.

KEYWORDS: Bio-oil, Hydrodeoxygenation, HZSM-5, Lignin, Ruthenium



INTRODUCTION

Bio-oils, sustainably produced from fast pyrolysis of abundant lignocellulosic biomass, have attracted global attention as a feedstock for the renewable production of biofuels.^{1–5} Currently, biofuels have been deemed to be a promising alternative to fossil fuels. Lignin is a phenol-based biopolymer showing a high energy density than cellulose and hemicelluloses among lignocellulosic biomass. Moreover, lignin is a rich source for phenolic bio-oils.⁶ Due to the large oxygen content, phenolic bio-oils, consisting of phenolic molecules such as phenol, guaiacol, syringol, and their derivatives, requires significant deoxygenation to convert into conventional transport alkane fuels. Therefore, phenolic compounds are generally regarded as important model compounds for bio-oil;^{4,7} whereas, hydrodeoxygenation was used for bio-oil upgrading.^{4,9} Sulfide catalysts such as cobalt- or nickel-doped molybdenum sulfides are currently used for hydrodeoxygenation purpose.^{3,10–15} An inherent drawback of these sulfide catalysts is the product contamination by sulfur transfer during upgrading process. An alternative approach based on nonsulfide catalysts, such as zeolite-supported nanocatalysts,^{16–20} Pt/C,²¹ Pd/C,^{22,23} Ni,^{16,24–27} and ionic liquid-stabilized nanocatalysts^{28,29} have been recently evaluated for hydrodeoxygenation purpose.

In the literature for the hydrodeoxygenation of lignin-derived phenols, Lercher^{16,17,22,23,25} and Kou^{22,25,28} made impressive progress on selective hydrodeoxygenation of lignin-derived phenolic monomers and dimers to cycloalkanes,^{17,22,23,25,28} as well as on upgrading of the crude bio-oil components in aqueous-phase.¹⁶ Zhang and co-workers achieved direct catalytic conversion raw lignocellulosic materials in an efficient way over a carbon supported Ni–W₂C catalyst.²⁷ Dyson et al. did nice work on hydrodeoxygenation of lignin-derived phenols into alkanes by using nanoparticle catalysts combined with Brønsted acidic ionic liquids.²⁸ Jones et al. developed an efficiently bifunctional catalyst of HY zeolite-supported Pt for the hydrodeoxygenation-hydrogenation-coupling of phenol in a fixed-bed reactor at elevated hydrogen pressure.¹⁸ Zhao et al. reported hydroalkylation and hydrodeoxygenation of phenol and substituted phenols to bicycloalkanes in a tandem reaction over Pd nanoclusters supported on a large-pore molecular sieve HBEA at 473–523 K using water as solvent.²⁰ Fukuoka reported hydrodeoxygenation of phenols as lignin models

Received: October 4, 2013

Revised: December 11, 2013

Published: December 26, 2013

under acid-free conditions with carbon-supported platinum catalysts.²¹ Resasco and co-workers investigated bifunctional transalkylation and hydrodeoxygenation of lignin model compounds over a Pt/HBeta catalyst.¹⁹

In addition to catalyst system, model compound researches are of also importance to establish a proper condition for efficient conversion of phenolic-rich feedstock.^{17,22,25,29} Besides the hydrodeoxygenation of phenolic monomers, the selective cleavage of the aromatic carbon–oxygen bonds in aryl ethers of lignin-derived phenolic dimers is also challenging.^{24,30,31}

Recently, we developed a new highly efficient one-pot route for hydrodeoxygenation of aqueous phenolics to cycloalkanes over a dual-functional catalyst system which combined the metal function of ionic liquid-like copolymer-stabilized ruthenium with a mineral acid.²⁹ However, the bottleneck for the industrial application of such a process is related to the catalyst recycling and an added mineral acid, leading to a relatively corrosive reaction environment. We thus thought it would be highly efficient and promising to construct an acid-metal bifunctional catalyst by supporting a transition metal on a solid acid support for hydrodeoxygenation purpose. Herein, we report on the use of acid–metal bifunctional catalyst, that is, a weaker solid acid of zeolite (HZSM-5)-supported ruthenium (Ru/HZSM-5), for the quantitative hydrodeoxygenation of diversely substituted lignin-derived mono- and binuclear phenols to cycloalkanes in aqueous solutions at a mild temperature (473 K). Recently, an optimum balance between acid and metal functions for bifunctional catalyst was revealed to achieve a maximum yield of desired product by Sels and us.^{32,33} Herein, the relationship between the acidity of HZSM-5 (in the term of Si/Al) and the selectivity of Ru/HZSM-5 to alkane products was investigated as well.

EXPERIMENTAL SECTION

Materials. Unless otherwise stated, all chemicals in this work were commercial available and used without further purification. 4-*n*-Propylguaiaicol was prepared by selective hydrogenation of eugenol according to the literature method.³⁴

Catalyst Preparation. All of the Pd, Pt, and Ru-loaded catalysts investigated in the hydrodeoxygenation were prepared by the conventional incipient wetness impregnation with the corresponding supports. For Ru/HZSM-5, the supported Ru catalysts were prepared by impregnating HZSM-5 with an aqueous solution of RuCl₃, the resultant suspension was stirred for 12 h at ambient temperature followed by evaporating excess water at 343 K. The solids remained were dried at 393 K under vacuum and calcined at 573 K for 3 h with a ramp of 10 K/min under the air. The catalysts were reduced at 523 K for 2 h with the heating rate of 10 K/min under 4 MPa H₂ before use. The prepared catalysts with different Si/Al molar ratios were denoted as Ru/HZSM-5 (Si/Al).

Catalytic Performance. The hydrodeoxygenation reactions were optimized by varying the noble metals (Pd, Pt, and Ru), the catalyst supports [Al₂O₃, SiO₂, HZSM-5 (Si/Al = 25, 38, 50, 150, 360)], and reaction parameter, such as temperature and time. The reaction conditions used are noted in the footnotes of the each table.

The hydrodeoxygenation reaction was carried out in a 60 mL stainless steel reactor equipped with a magnetic stirrer. In a typical experiment, phenol (200 mg, 2.13 mmol) or other lignin-derived monomers or dimers (2.0 mmol) and catalyst were added to 10 mL water in the stainless steel reactor. After purging the reactor three times with hydrogen, the outlet valve was then closed to maintain 5.0 MPa of hydrogen pressure (ambient temperature). Reactions were conducted at 473 K for 4 h with a stirring speed of 600 rpm. After the reaction was halted, the reactor was cooled to room temperature. Ethyl acetate was used to extract the organic mixture and the aqueous phase was also collected. The organic phase and aqueous phase were both

analyzed by a gas chromatograph (GC) and gas chromatograph–mass spectrometer (GC-MS).

RESULTS AND DISCUSSION

Hydrodeoxygenation of Phenol over HZSM-5-Supported Metal Catalyst. An initial experiment was carried out to investigate the effect of the metal sites on the hydrodeoxygenation of phenol at 423 K. A series of noble metals supported on HZSM-5 (Si/Al = 38) were evaluated as catalysts for aqueous-phase hydrodeoxygenation of phenol; the Ru is more active and selective to afford cyclohexane than Pd and Pt as shown in Table 1 (entries 1–2 and 6). This result can be

Table 1. Aqueous-Phase Hydrodeoxygenation of Phenol^a

entry	catalyst M/HZSM-5(Si/Al)	conversion [%]	selectivity [%]	
			cyclohexane	cyclohexanol
1	Pd/HZSM-5(38)	99.9	73.5	24.3
2	Pt/HZSM-5(38)	99.9	68.6	28.6
3	Ru/HZSM-5(360)	99.9	0.4	97.1
4	Ru/HZSM-5(150)	99.9	0.7	96.9
5	Ru/HZSM-5(50)	99.9	14.4	83.0
6	Ru/HZSM-5(38)	99.9	87.2	9.9
7	Ru/HZSM-5(25)	99.9	96.3	0.2
8	Ru/SiO ₂	99.9	0.4	96.8
9	Ru/Al ₂ O ₃	99.9	0.1	97.6

^aReaction conditions: phenol (200 mg, 2.13 mmol), catalyst (100 mg, metal loading 1.0 wt %), water (10 mL), P_{H₂} (5 MPa), T (423 K), t (2 h).

attributed to the higher hydrogenolysis activity of Ru.³⁵ Moreover, the price advantage of Ru over Pd and Pt raises a potential application purpose for the developed Ru/HZSM-5.

In addition to metallic sites, the Si/Al ratio has been shown to be a critical factor in determining the acid strength as well as hydrophobicity of the catalyst. We thus explored the effect of the Si/Al ratio of HZSM-5 support in the hydrodeoxygenation of phenol as described by the data in Table 1. The conversions of phenol, exceeding 99.9% under all investigated conditions, did not depend on the Si/Al ratio and topology of the zeolite used. Moreover, all catalysts displayed high activity to phenol hydrogenation (Table 1, entries 3–7). However, the selectivity to cyclohexane steeply increased with the decreasing Si/Al ratio of HZSM-5, with a significant rise to 96.3% of cyclohexane selectivity for a Si/Al ratio of 25 (Table 1, entry 7). On the other hand, the selectivity to cyclohexanol sharply decreased with Si/Al ratio of HZSM-5 (Table 1, entries 3–7). The dehydration of cyclohexanol was further investigated over pure HZSM-5 (Supporting Information Table S1). As expected, the conversion of cyclohexanol to cyclohexene decreased with the increasing Si/Al ratio of HZSM-5, indicating that HZSM-5 support with lowest Si/Al ratio is beneficial for the dehydration of cyclohexanol. Moreover, in the case of HZSM-5(25)-promoted cyclohexanol dehydration, a trace amount of dicyclohexyl ether was observed through the pathway of intermolecular dehydration of cyclohexanol (Supporting Information Table S1, entry 1). The above result indicates that the catalyst Ru/HZSM-5 with the lowest Si/Al ratio of HZSM-5 proved to be most selective to cyclohexane, which is consistent with more efficient dehydration.

In the cases of Ru/SiO₂ and Ru/Al₂O₃ catalysts containing the support of negligible acidity and nonporous structure, the

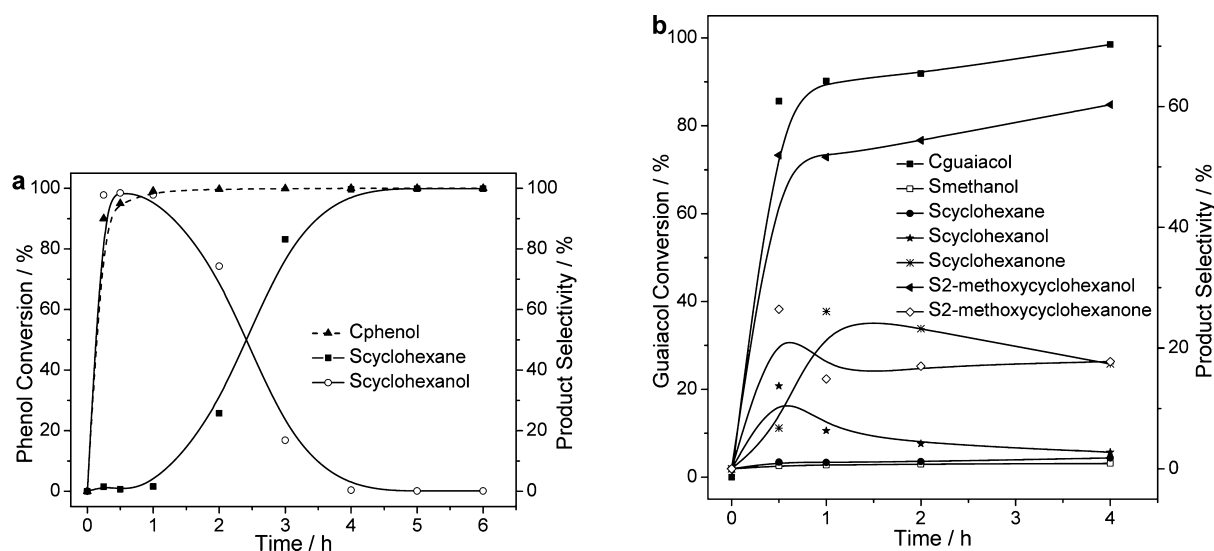


Figure 1. Product distributions of hydrodeoxygenation of phenol (a) and guaiacol (b) as a function of reaction time in aqueous-phase. Reaction conditions: phenol (200 mg, 2.13 mmol) or guaiacol (265 mg, 2.13 mmol), Ru/HZSM-5 (100 mg, Ru 1 wt %, Si/Al = 25), water (10 mL), T (413 K), P_{H_2} (5 MPa).

main products were cyclohexanol and subsequent reaction of dehydration was not observed (Table 1, entries 8–9). This result implies that the presence of dual catalytic functions is indispensable for the formation of cyclohexane from phenol through hydrodeoxygenation process.³⁶ Hydrogenation of phenol on Ru leads to cyclohexanol as the initial product. Its dehydration in water is catalyzed by Brønsted acid site in the pores of HZSM-5.

NH₃-TPD Study on Catalyst. The temperature programmed desorption of ammonia (NH₃-TPD) profiles for pure HZSM-5 and Ru/HZSM-5 (Ru 1 wt %) were shown in Supporting Information Figures S1 and S2, respectively. In the NH₃-TPD curves of HZSM-5, peaks are generally observed in two temperature regions referred to as low-temperature and high-temperature region, respectively (Figure S1). Moreover, both peak areas and maximum temperatures for each profile reduce significantly with an increasing Si/Al ratio from 25 to 360, indicating the reduced acid amount and strength with an increasing Si/Al ratio (Figure S1). The formation of ruthenium nanoparticles on HZSM-5 could, however, result in pore blockage leading to the reduction of the amount of active acid sites of Ru/HZSM-5 compared with pure HZSM-5 (Figures S1 and S2). As shown in Figure S2, two desorption peaks were observed over the Ru/HZSM-5, the one at 555–628 K was attributed to weak adsorption of NH₃ over the Brønsted acid site, corresponding to NH₃ association with Si–OH.³⁷ The other peak at 727–827 K was ascribed to strong desorption of adsorbed NH₃ on the acidic Si–OH–Al group (Figure S2a–c).³⁸ A broad peak of NH₃ desorption at a lower temperature was observed for the catalyst Ru/HZSM-5 with a higher Si/Al ratio of 360 (Figure S2a). A shift of desorption peaks toward higher temperature was observed over the Ru/HZSM-5 catalyst as the decrease of the Si/Al ratio (Figure S2a–c), indicating a stronger interaction between NH₃ and the acid sites of HZSM-5 support.^{39,40} The NH₃-TPD results further proved the tendency in Table 1 (entries 3–9), indicating that the stronger acidity of zeolite may cause dehydration and lead to higher selectivity to hydrocarbons.

Effects of the Reaction Parameter on Hydrodeoxygenation of Phenol. The influences of reaction temperature and

time on the hydrodeoxygenation of phenol into cyclohexane with Ru/HZSM-5 as catalyst were shown in Supporting Information Table S2. An initial experiment was carried out at 373 K, and the conversion of phenol was 99.9%; however, even with a prolonged reaction time to 24 h, the predominant product was cyclohexanol rather than cyclohexane (Table S2, entries 1–2). It was also found that temperature dramatically affected the formation of cyclohexane and the selectivity of cyclohexane increased from 1.2 to 98.1% in the temperature range from 373 to 473 K; whereas, the selectivity of cyclohexanol decreased from 95.1 to 0.1% (Table S2). Moreover, the times needed for a maximum selectivity of cyclohexane are different, based on the different reaction temperatures; that is, the higher the temperature is, the shorter the reaction time needs to be. These results indicate that the dehydration step is highly temperature-dependent and the rate-determining step for the phenol hydrodeoxygenation, which is in accordance with the reported results.^{23,29}

Catalyst Recycling. To test for catalyst recyclability, a batch of Ru/HZSM-5 (Ru 1.0 wt %, Si/Al = 25) catalyst was repeatedly used on the phenol hydrodeoxygenation at 473 K and 5 MPa H₂ for 1 h. It is important to highlight that nearly identical results were achieved after three recycles (Supporting Information Table S3, entries 1–3). No changes regarding the conversion of phenol and only slightly reduced selectivity toward cyclohexane were observed respect to the fresh catalyst. Moreover, catalyst recycling was performed at 373 K for 0.5 h with a low level of phenol conversion as well to obtain a further insight into the mechanism. Under the above conditions, phenol conversions slightly reduced from 44.9 to 40.7%, the selectivities of cyclohexanol slightly reduced from 94.3 to 91.9% after four recycles (Table S3, entries 4–7). The above results further suggest that the dehydration step is highly temperature-dependent and catalyst Ru/HZSM-5 is recyclable. Moreover, the expected cyclohexanone product was unobserved and only trace amount of cyclohexene was obtained, indicating that the phenol hydrodeoxygenation goes through a cyclohexanol intermediate rather than cyclohexanone. On the basis of NH₃-TPD analysis, the desorption curves of NH₃ over recycled catalyst Ru/HZSM-5 (Supporting Information Figure S2d)

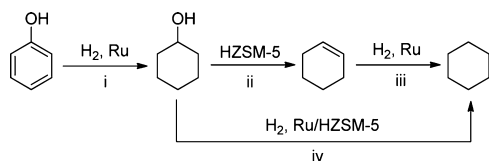
shows a shift of strong NH_3 desorption peak toward lower temperature than the fresh one (Figure S2c), presumably due to a strong adsorption of phenol in the pore of recovered HZSM-5. Inductively coupled plasma-atomic emission spectroscopy (ICP-AES) analysis of the organic phase and the aqueous solution after each cycle did not show even traces of leached Ru.

Hydrodeoxygenation Profiles of Phenol and Guaiacol.

To probe the stepwise aqueous-phase hydrodeoxygenation of phenols over Ru/HZSM-5, phenol and guaiacol were selected as model compounds. Figure 1a plots the aqueous phase conversion of phenol at 413 K with Ru/HZSM-5 as catalyst versus reaction time. It can be seen that both the selectivity of cyclohexanol and phenol conversion increased steeply during an initial 15 min. After 30 min, the reaction progress was accompanied by an increase in cyclohexane selectivity and a decrease in cyclohexanol selectivity. Cyclohexane was obtained quantitatively after 5 h. Notably, these results were, however, inconsistent with Pd/C- H_3PO_4 system-catalyzed phenol hydrodeoxygenation, in which phenol is hydrogenated to cyclohexanone in the first step and then to cyclohexanol.^{22,23} In our case, the “intermediate” cyclohexanone was unobserved under the investigated conditions.

Recently, Tomishige and co-workers reported high yields of *n*-hexane production from hydrogenolysis of aqueous sorbitol using Ir- $\text{ReO}_x/\text{SiO}_2$ catalyst combined with HZSM-5 as a cocatalyst.⁴¹ Moreover, the authors further proved that Ru catalyst were more active in the C–O hydrogenolysis of glycerol than Pt and Pd compounds.⁴² Therefore, in our case, a reaction pathway of direct cyclohexanol hydrogenolysis over Ru/HZSM-5 to give cyclohexane might also be involved in the phenol hydrodeoxygenation (Scheme 1).

Scheme 1. Proposed Reaction Pathway for Hydrodeoxygenation of Phenol



The elementary reactions for phenol hydrodeoxygenation over Ru/HZSM-5 in the aqueous-phase thus are divided into the following three processes (Scheme 1), (i) direct phenol hydrogenation to cyclohexanol over Ru/HZSM-5, (ii) cyclohexanol dehydration to cyclohexene over HZSM-5, and (iii) cyclohexene hydrogenation to cyclohexane over Ru/HZSM-5. Moreover, (iv) a direct cyclohexanol hydrogenolysis to cyclohexane over Ru/HZSM-5 might be another elementary reaction involved in phenol hydrodeoxygenation (Scheme 1). Table 2 shows the turnover frequencies (TOFs) for the hydrogenation of above network. The TOF of phenol hydrogenation over Ru/HZSM-5 was $118 \text{ mol}_{\text{phenol}} \text{ mol}_{\text{Ru}}^{-1} \text{ h}^{-1}$ at 393 K under a low phenol conversion level of 10% (Table 2). Under the above conversions, cyclohexanol was observed to be the predominant product with a selectivity of 86.5%. The rate of cyclohexanol dehydration over HZSM-5 was about $15 \text{ mol}_{\text{cyclohexanol}} \text{ mol}_{\text{NH}_3}^{-1} \text{ h}^{-1}$ with observed selectivity of 99.9% to cyclohexene. The TOF rate of cyclohexene hydrogenation to cyclohexane over Ru/HZSM-5 was $2.1 \times 10^3 \text{ mol}_{\text{cyclohexene}} \text{ mol}_{\text{Ru}}^{-1} \text{ h}^{-1}$, a far higher value than that of the phenol hydrogenation. In the case of cyclohexanol conversion,

Table 2. Turnover Frequencies for the Network of Phenol Hydrodeoxygenation over Ru/HZSM-5

process over Ru/HZSM-5 or HZSM-5	TOF [$\text{mol}_{\text{sub}} \text{ mol}_{\text{Ru}}^{-1} \text{ h}^{-1}$] ^{a,c} or [$\text{mol}_{\text{sub}} \text{ mol}_{\text{NH}_3}^{-1} \text{ h}^{-1}$] ^b
(i) phenol hydrogenation ^a	118
(ii) cyclohexanol dehydration ^b	15
(iii) cyclohexene hydrogenation ^a	2.1×10^3
(iv) cyclohexanol hydrogenolysis ^a	7
(i) phenol hydrogenation ^{a,c}	1.3×10^4

^aReaction conditions: substrate (2.13 mmol), Ru/HZSM-5 (40 mg, Ru 1 wt %, Si/Al = 25), water (10 mL), P_{H_2} (5 MPa), T (393 K).

^bCyclohexanol (2.13 mmol), HZSM-5 (40 mg, Si/Al = 25), water (10 mL), P_{N_2} (5 MPa), T (393 K). ^c T (473 K) was used instead of 393 K.

the rate of cyclohexanol hydrogenolysis was extremely inferior over Ru/HZSM-5; the obtained TOF values were about $7 \text{ mol}_{\text{cyclohexanol}} \text{ mol}_{\text{Ru}}^{-1} \text{ h}^{-1}$ with observed selectivity of 52.3% to cyclohexane. Notably, the TOF rate of phenol hydrogenation is highly temperature-dependent; the observed TOF value for phenol hydrogenation over Ru/HZSM-5 was $1.3 \times 10^4 \text{ mol}_{\text{phenol}} \text{ mol}_{\text{Ru}}^{-1} \text{ h}^{-1}$ at 473 K, which is in sharp contrast to the TOF value of $118 \text{ mol}_{\text{phenol}} \text{ mol}_{\text{Ru}}^{-1} \text{ h}^{-1}$ at 393 K.

As shown in Table 3, the hydroxyl (–OH) and methoxy (–OCH₃) are the major functional groups of lignin derived phenolics. Therefore, guaiacol (2-methoxyphenol) with adjacent methoxy and hydroxy functional groups at the aromatic ring is a typical phenolic model compound, which also represents a thermal conversion product of biomass lignin.¹⁹ In addition to phenol, the catalytic hydrodeoxygenation of guaiacol was investigated as well over Ru/HZSM-5 at 413 K (Figure 1b). It can be seen that, under low temperature hydrodeoxygenation of guaiacol, 2-methoxycyclohexanol is, however, the predominant product with a selectivity of more than 50%. In the case of Pd/C- H_3PO_4 system-catalyzed guaiacol hydrodeoxygenation, 2-methoxycyclohexanone was primary product.²³ Moreover, both the 2-methoxycyclohexanol selectivity and guaiacol conversion increased steeply over Ru/HZSM-5 at an initial 30 min. Three species of 2-methoxycyclohexanone, cyclohexanone, and cyclohexanol were observed to be formed and later gradually consumed in the interval of time, suggesting an intermediate behavior under the investigated conditions. The selectivity of cyclohexane increased slowly with guaiacol conversion. Moreover, the facts that 2-methoxycyclohexanol shows a higher selectivity than 2-methoxycyclohexanone at all reaction times investigated and 2-methoxycyclohexanone shows a higher initial concentration over cyclohexanone suggest that the fastest step is the metal-catalyzed hydrogenation of the aromatic ring in guaiacol rather than the acid-catalyzed hydrolysis of the methoxy group. In comparison with phenol, guaiacol has an adjacent methoxy group. Therefore, the observed incomplete hydrogenation product of 2-methoxycyclohexanone can presumably be related to electron donation by the adjacent methoxy group, preventing its further hydrogenation.

Hydrodeoxygenation of Monomeric Model Compounds. In an extension to phenol, a series of monomeric lignin model compounds were efficiently converted into alkanes using Ru/HZSM-5(25) as a bifunctional catalyst under the optimized hydrodeoxygenation conditions (473 K, 5 MPa H_2 , 4 h) as shown in Table 3. In the cases of representative bioderived phenolic monomers, anisole, catechol, and guaiacol were quantitatively converted to hydrocarbons with the

Table 3. Hydrodeoxygenation of Phenolic Monomers over Ru/HZSM-5^a

entry	substrates	conversion [%]	selectivity [%]				
	C6 backbone						CH ₃ OH
1		>99.9	93.4	0.1	0.1	/	2.1
2		>99.9	95.7	/	0.1	0.2	/
3		>99.9	93.6	/	0.1	/	1.7
4		76.2	57.2	12.4	6.8	14.6	4.4
	C7						
5		>99.9					
			>97.4				
6		99.8					CH ₃ OH 1.3
			85.6	4.0	0.8	5.6	
	C8						
7		>99.9					CH ₃ OH 1.4
			85.2	3.5	1.4	2.3	
	C9						
8		>99.9					
			95.1	0.9	0.5		
9		99.6				CH ₃ OH 1.2	
			89.5	4.5	1.4		
10		>99.9				CH ₃ OH 1.3	
			85.4	3.7	5.2		

^aReaction conditions: phenolic monomer (2.0 mmol), Ru/HZSM-5 (135 mg, Ru 1.0 wt %, Si/Al = 25), water (10 mL), P_{H_2} (5 MPa), T (473 K), t (4 h).

cyclohexane yields ranging from 93.4 to 95.7% under the investigated conditions (Table 3, entries 1–3). In sharp contrast, this catalyst Ru/HZSM-5, however, showed moderate activity (76.2% conversion) with syringol (2,6-dimethoxyphenol) at 473 K (Table 3, entry 4), implying that the two methoxy groups increase steric effect, stabilize the aromatic ring, and increase the difficulty for hydrogenation.

Moreover, phenolic monomers, containing seven to nine carbon atoms directly linked in the backbone, were investigated as well. In most cases, the one-pot aqueous phase process led to over 89% yields of hydrocarbons, being highly atom economic and energy efficient (Table 3, entries 5–10). In addition, these hydrocarbon products, produced from the bifunctional catalyst, were mainly saturated alkanes as shown in Table 3, further emphasizing high hydrogenation activity of the catalyst Ru/HZSM-5.

Due to weak acidity of the support HZSM-5 (Si/Al = 25), acid catalyzed skeletal isomerization (ring contraction) products derived from cycloalkane, such as 1,3-dimethylcyclopentane, ethylcyclopentane, 1-ethyl-3-methylcyclopentane, and 1-*n*-propyl-2-methylcyclopentane were obtained for the C7–C9 backbone phenolic-monomer conversion, with

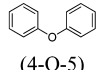
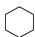
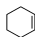
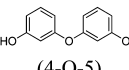
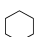
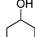
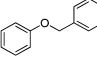
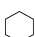
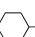
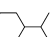
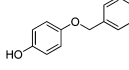
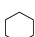
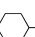
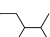
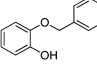
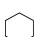
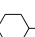
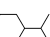
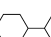
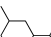
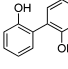
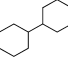
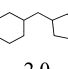
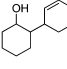
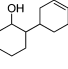
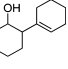
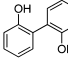
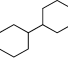
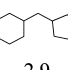
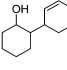
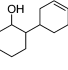
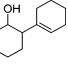
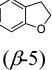
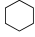
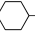
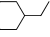
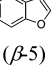
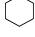
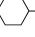
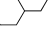
selectivities from 0.8 to 4.0% (Table 3, entries 6–8). Similarly, a skeletal isomerization product of 1-ethyl-3-methylcyclohexane from 2-methoxy-4-*n*-propylphenol and eugenol (4-allyl-2-methoxyphenol) was observed as well (Table 3, entries 8–10). Moreover, in these reactions, the methoxy group was hydrolyzed or hydrogenolyzed to give methanol in 1.3–3.3% yields.^{17,22,23,25,29}

Notably, with a comparable or even higher catalytic performance, the hydrodeoxygenation temperature is 473 K for Ru/HZSM-5, which is remarkably low than in the cases of Ru/copolymer–H₃PO₄ (513 K),²⁹ Pd/C–H₃PO₄ (523 K),^{22,23} Raney Ni–Nafion/SiO₂ (573 K),²⁵ Pt/AC (553 K),²¹ and Pt/HBeta (673 K),¹⁹ Pt/HY (523 K),⁴³ Ni–Mo/ γ -Al₂O₃ (553 K),^{44–46} and Ni–Cu/CeO₂ (573 K).⁴⁷ These results thus indicate that the new catalytic approach with the developed bifunctional catalyst of Ru/HZSM-5 can be effectively applied in the hydrodeoxygenation of the diverse substituted phenolic monomers.

Hydrodeoxygenation of Dimeric Model Compounds.

To explore the scope of the application of the Ru/HZSM-5 catalyst, we further investigated the hydrodeoxygenation of more complicated bioderived phenolic dimers under the same

Table 4. Hydrodeoxygenation of Phenolic Dimers over Ru/HZSM-5^a

entry	substrates	conversion [%]	selectivity [%]				
1	 (4-O-5)	99.8					
			96.8	0.3			
2	 (4-O-5)	99.8					
			97.4	0.1			
3	 (α -O-4)	99.9					
			34.5	48.8	13.1		
4	 (α -O-4)	99.9					
			38.6	50.4	6.7		
5	 (α -O-4)	99.9					
			25.8	33.5	2.1	15.1	20.5
6	 (5-5')	99.8					
			50.2	2.0	10.8	22.7	9.3
7 ^b	 (5-5')	99.8					
			77.8	2.9	3.0	1.9	7.1
8	 (β -5)	99.3					
			5.4	28.6	61.4		
9	 (β -5)	99.9					
			3.8	22.6	70.4		

^aReaction conditions: phenolic dimer reactant (2.0 mmol), Ru/HZSM-5 (135 mg, Ru 1.0 wt %, Si/Al = 25), water (10 mL), P_{H_2} (5 MPa), T (473 K), t (4 h). ^bThe hydrodeoxygenation reaction was performed at 493 K instead of 473 K.

conditions. Typically, the model compounds shown in Table 4 were chosen to represent 4-O-5 (entries 1–2), α -O-4 (entries 3–5), β -5 phenylcoumaran (entries 8–9) ether linkages and the 5–5' aryl–aryl linkage (entry 6), which can be found in the lignin structure. As can be seen, >99% conversions of phenolic dimers were achieved in all cases, and the overall selectivities to alkanes were excellent (>96%; Table 4, entries 1–5 and 8–9) to good (>84%; Table 4, entry 7).

The 4-O-5 dimers diphenyl ether (DPE) and 3,3'-dihydroxy-substituted DPE were quantitatively converted to C6 cyclohexane over Ru/HZSM-5 at 473 K and 5 MPa H_2 (Table 4, entries 1–2). By comparison, the previously explored catalysts of Ru/copolymer- H_3PO_4 required 513 K to efficiently hydrodeoxygenate DPE and dihydroxy-substituted DPE to cyclohexane,²⁹ again showing that Ru/HZSM-5 is a more efficient catalyst. Moreover, DPE was found to remain unchanged using only HZSM-5 (Si/Al = 25) as catalyst at same hydrothermal conditions, suggesting that synergistic effect between Ru and HZSM-5 might be involved in the bifunctional catalyst system.

The benzyloxybenzene (α -O-4) and the *p*- or *o*-hydroxy-substituted α -O-4 model compounds were also quantitatively converted to C6–C10 alkanes under these conditions (Table 4, entries 3–5). This result was, however, inconsistent with the dual catalyst system of Pd/C and HZSM-5 (Si/Al = 45), in

which only C6 cyclohexane and C7 methylcyclohexane were obtained as hydrocarbons.¹⁷ Previous work has shown that the methyl in the methoxyl of phenolics could be transferred to the aromatic ring through acid catalyzed transalkylation reactions over HZSM-5.⁴⁸ Therefore, the formation of C8–C10 alkanes in our case was presumably due to the acid catalyzed transalkylation reactions over HZSM-5 (Si/Al = 25) followed by subsequent isomerization of substituted cyclohexanes on the stronger Brønsted acid sites of HZSM-5. This result indicates that the product distribution of liquid oil during the upgrading of phenolics-containing bio-oils can be controlled by adjusting the metal/acid balance.^{32,33}

The compounds 2,2'-biphenol (Table 4, entry 6), coumaran (dihydrobenzofuran, Table 4, entry 8), and benzofuran (Table 4, entry 9) represent some key features of the 5–5' and the phenylcoumaran-type linkages encountered in lignin.^{6,10} For 2,2'-biphenol, in addition to a 50% yield of expected 1,1'-bi(cyclohexane), an about 43% yield of the cyclohexenyl-substituted cyclohexanol intermediates were also detected after 4 h reaction time at 473 K, suggesting that the hydrogenation rate of 2,2'-biphenol is considerably lower than those of other dimers (Table 4, entry 6). This may be attributed to the fact that the intramolecular hydrogen bonds in 2,2'-biphenol could hinder the attack of the catalyst.⁴⁹ Moreover, a phenolic hydroxyl group, a strongly hydrogen-bridging interacting

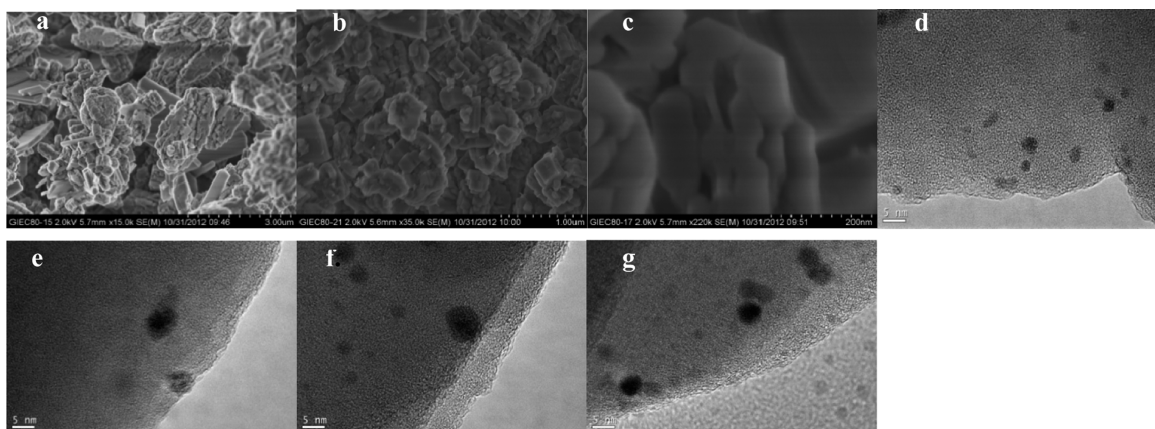


Figure 2. (a) SEM micrographs of an HZSM-5 (Si/Al = 25); (b, c) SEM and (d) TEM micrographs of fresh Ru/HZSM-5 (Ru 1.0 wt %, Si/Al = 25) at different magnifications; (e) TEM micrographs of recovered Ru/HZSM-5 after four recycles with the reaction conditions described in Supporting Information Table S3 run 4; TEM micrographs of Pd/HZSM-5 (f) and Pt/HZSM-5 (g), (Pd and Pt, 1.0 wt %, Si/Al = 25).

system,^{50–52} can presumably interact strongly with a Si–OH–Al group on the HZSM-5 surface through hydrogen bonds to form strong O–H...O–Si(Al) interactions. Therefore, the existence of the incomplete hydrodeoxygenation product cyclohexenyl-substituted cyclohexanols may also be attributed to relatively strong adsorption of 2,2'-biphenol on the surface of HZSM-5. Both excellent conversion of 2,2'-biphenol (99.8%) and good selectivity to alkanes (83.5%) could still be reached with an increased reaction temperature to 493 K (Table 4, entry 7).

Both dihydrobenzofuran and benzofuran are common probe molecules for hydrodeoxygenation reactions⁵³ and can serve as β -5 linkage model compounds that resemble phenylcoumaran linkages in lignin.²³ After reacting over a Ru/HZSM-5 catalyst for 4 h at 473 K and 5 MPa hydrogen pressure, >99% of both the dihydrobenzofuran and benzofuran were converted. As can be seen in Table 4 (entries 8–9), high selectivity toward alkanes is achieved; moreover, ethylcyclohexane, obtained by hydrogenation of aromatic ring followed by dehydration and hydrogenation reactions, is predominant deoxygenated product. The above results about hydrodeoxygenation of dimeric model compounds suggest that the one-pot approach with Ru/HZSM-5 can be applied for widely diverse phenolic dimer conversion.

Catalyst Characterization. To identify the active species for the hydrogenation, X-ray powder diffraction (XRD) analysis was performed for Ru/HZSM-5. However, no diffraction peaks corresponding to Ru crystallite can be observed over the catalyst (Supporting Information Figure S3), which indicates that highly dispersed Ru species exist in the very small nanoparticle or in amorphous structure. Moreover, the XRD patterns of recovered Ru/HZSM-5 show some slight variations than the fresh one, indicating partial loss of crystallinity in the support HZSM-5 for the recovered catalyst (Supporting Information Figure S3). The Brunauer–Emmett–Teller (BET) surface analysis indicates that the specific surface area significantly decreases from 254 m² g⁻¹ for the fresh Ru/HZSM-5 to 204 m² g⁻¹ for the recovered one (Supporting Information Figure S4), further suggesting a change in zeolite crystallinity or adsorption of phenol in the pore after the reuse of Ru/HZSM-5 under hydrothermal conditions.

Figure 2 shows the scanning electron microscopy (SEM) and transmission electron microscopy (TEM) images of Ru/HZSM-5 catalyst. SEM observations of the HZSM-5 zeolite

show well ordered and uniform crystallites with a quasi-spherical shape (Figure 2a). The pure HZSM-5 presented as a relatively smooth surface with the size of several micrometers. With the Ru loading, the size of HZSM-5 remained almost unchanged, and the Ru particles were hardly seen, which were due to the small particles size and high dispersion of Ru particles on the HZSM-5 surface (Figure 2b–c). This result was well consistent with XRD patterns (Supporting Information Figure S3). Figure 2d shows the typical TEM images for Ru loaded on HZSM-5 sample. Analysis of this Ru fraction showed that the average Ru particle size of 2.3 nm with a dispersion of 28.4% according to the equations reported by Van Der Grift et al.⁵⁴ However, the recovered Ru catalyst after four-time recycling (Table S3, run 4–7) had average particle sizes of 4.0 nm (Figure 2e). Therefore, the slightly reduced phenol conversions in the catalyst recycling as described in Table S3 was presumably related to the increase in average particle size of recovered Ru nanoparticles and partial loss of crystallinity of support HZSM-5. In the case of catalysts Pd/HZSM-5 and Pt/HZSM-5 (Pd and Pt, 1.0 wt %, Si/Al = 25), TEM analyses show average particle size of 6.0 nm for Pd (Figure 2f) and 3.3 nm for Pt (Figure 2g).

Ru/HZSM-5 was evaluated further by X-ray photoelectron spectroscopy (XPS). The XPS elemental survey scans of the surface of the Ru/HZSM-5 show peaks corresponding to oxygen, ruthenium, aluminum, and silicon (Supporting Information Figure S5a). The XPS spectrum of Ru3d can be deconvoluted into two peaks with the binding energies of 280.1 eV (assigned to Ru3d5/2) and 286.0 eV (assigned to Ru3d3/2), as illustrated in Figure S5b. The binding energy of the Ru3d5/2 level in the Ru/HZSM-5 is 0.1 eV lower than that of the standard zerovalent state of Ru (280.2 eV),⁵⁵ indicating that the Ru³⁺ ion was successfully reduced to Ru⁰ state in Ru/HZSM-5.

CONCLUSIONS

In summary, the acid-metal bifunctional catalyst Ru/HZSM-5 (Si/Al = 25) showed a high selectivity in removing oxygen-containing groups from lignin-derived phenolic monomers and dimers in water at 473 K. Our result also indicates that the presence of dual catalytic functions of Ru/HZSM-5 is indispensable for the formation of alkanes from lignin-derived phenolics through hydrodeoxygenation process, i.e., both the presence of Brønsted acid site in the pores of HZSM-5 for

dehydration and a metallic function of Ru for hydrogenation were needed. Moreover, the dehydration step is highly dependent on both the acidity of the support HZSM-5 and reaction temperature. This approach for the construction of bifunctional catalyst opens an efficient route for hydrodeoxygenation of lignin-derived phenolic oil to transportation biofuels.

■ ASSOCIATED CONTENT

● Supporting Information

Experimental details, Tables S1–S3, and Figures S1–S5. This material is available free of charge via the Internet at <http://pubs.acs.org>.

■ AUTHOR INFORMATION

Corresponding Author

*Tel./Fax: (+86)-20-3722-3380. E-mail address: chenjz@ms.giec.ac.cn.

Notes

The authors declare no competing financial interest.

■ ACKNOWLEDGMENTS

We are grateful for the financial support from National Natural Science Foundation of China (21172219, 21207039, and 21250110061), National Basic Research Program of China (973 Program, 2012CB215304), and Guangdong Natural Science Foundation (S2013010012986, S2011010002274, and S2013040012615).

■ REFERENCES

- (1) Kunkes, E. L.; Simonetti, D. A.; West, R. M.; Ruiz, J. C. S.; Gärtner, C. A.; Dumesic, J. A. Catalytic conversion of biomass to monofunctional hydrocarbons and targeted liquid-fuel classes. *Science* **2008**, *322*, 417–421.
- (2) Stöcker, M. Biofuels and biomass-to-liquid fuels in the biorefinery: Catalytic conversion of lignocellulosic biomass using porous materials. *Angew. Chem., Int. Ed.* **2008**, *47*, 9200–9211.
- (3) Elliott, D. C. Historical developments in hydroprocessing bio-oils. *Energy Fuels* **2007**, *21*, 1792–1815.
- (4) Huber, G. W.; Iborra, S.; Corma, A. Synthesis of transportation fuels from biomass: chemistry, catalysts, and engineering. *Chem. Rev.* **2006**, *106*, 4044–4098.
- (5) Mohan, D.; Pittman, C. U.; Steele, P. H. Pyrolysis of wood/biomass for bio-oil: A critical review. *Energy Fuels* **2006**, *20*, 848–889.
- (6) Zakzeski, J.; Bruijninx, P. C.; Jongerius, A. A. L.; Weckhuysen, B. M. The catalytic valorization of lignin for the production of renewable chemicals. *Chem. Rev.* **2010**, *110*, 3552–3599.
- (7) Crossley, S.; Faria, J.; Shen, M.; Resasco, D. E. Solid Nanoparticles that catalyze biofuel upgrade reactions at the water/oil interface. *Science* **2010**, *327*, 68–72.
- (8) Jae, I.; Tompsett, G. A.; Lin, Y. C.; Carlson, T. R.; Shen, I.; Zhang, T.; Yang, B.; Wyman, C. E.; Conner, W. C.; Huber, G. W. Depolymerization of lignocellulosic biomass to fuel precursors: maximizing carbon efficiency by combining hydrolysis with pyrolysis. *Energy Environ. Sci.* **2010**, *3*, 358–365.
- (9) Czernik, S.; Bridgwater, A. V. Overview of applications of biomass fast pyrolysis oil. *Energy Fuels* **2004**, *18*, 590–598.
- (10) Jongerius, A. L.; Jastrzebski, R.; Bruijninx, P. C. A.; Weckhuysen, B. M. CoMo sulfide-catalyzed hydrodeoxygenation of lignin model compounds: An extended reaction network for the conversion of monomeric and dimeric substrates. *J. Catal.* **2012**, *285*, 315–323.
- (11) Lin, Y. C.; Li, C. L.; Wan, H. P.; Lee, H. T.; Liu, C. F. Catalytic hydrodeoxygenation of guaiacol on Rh-based and sulfided CoMo and NiMo catalysts. *Energy Fuel* **2011**, *25*, 890–896.
- (12) Ryymin, E. M.; Honkela, M. L.; Viljava, T. R.; Krause, A. O. I. Insight to sulfur species in the hydrodeoxygenation of aliphatic esters over sulfided NiMo/ γ -Al₂O₃ catalyst. *Appl. Catal. A Gen.* **2009**, *358*, 42–48.
- (13) Ryymin, E. M.; Honkela, M. L.; Viljava, T. R.; Krause, A. O. I. Competitive reactions and mechanisms in the simultaneous HDO of phenol and methyl heptanoate over sulphided NiMo/ γ -Al₂O₃. *Appl. Catal. A Gen.* **2010**, *389*, 114–121.
- (14) Furimsky, E. Catalytic hydrodeoxygenation. *Appl. Catal. A Gen.* **2000**, *199*, 147–190.
- (15) Elliott, D. C.; Beckman, D.; Bridgwater, A. V.; Diebold, J. P.; Gevert, S. B.; Solantausta, Y. Developments in direct thermochemical liquefaction of biomass: 1983–1990. *Energy Fuels* **1991**, *5*, 399–410.
- (16) Zhao, C.; Lercher, J. A. Upgrading pyrolysis oil over Ni/HZSM-5 by cascade reactions. *Angew. Chem., Int. Ed.* **2012**, *51*, 5935–5940.
- (17) Zhao, C.; Lercher, J. A. Selective hydrodeoxygenation of lignin-derived phenolic monomers and dimers to cycloalkanes on Pd/C and HZSM-5 catalysts. *ChemCatChem* **2012**, *4*, 64–68.
- (18) Hong, D.-Y.; Miller, S. J.; Agrawal, P. K.; Jones, C. W. Hydrodeoxygenation and coupling of aqueous phenolics over bifunctional zeolite-supported metal catalysts. *Chem. Commun.* **2010**, *46*, 1038–1040.
- (19) Zhu, X. L.; Lobban, L. L.; Mallinson, R. G.; Resasco, D. E. Bifunctional transalkylation and hydrodeoxygenation of anisole over a Pt/HBeta catalyst. *J. Catal.* **2011**, *281*, 21–29.
- (20) Zhao, C.; Camaioni, D. M.; Lercher, J. A. Selective catalytic hydroalkylation and deoxygenation of substituted phenols to bicycloalkanes. *J. Catal.* **2012**, *288*, 92–103.
- (21) Ohta, H.; Kobayashi, H.; Hara, K.; Fukuoka, A. Hydrodeoxygenation of phenols as lignin models under acid-free conditions with carbon-supported platinum catalysts. *Chem. Commun.* **2011**, *47*, 12209–12211.
- (22) Zhao, C.; Kou, Y.; Lemonidou, A. A.; Li, X.; Lercher, J. A. Highly selective catalytic conversion of phenolic bio-oil to alkanes. *Angew. Chem., Int. Ed.* **2009**, *48*, 3987–3990.
- (23) Zhao, C.; He, J. Y.; Lemonidou, A. A.; Li, X. B.; Lercher, J. A. Aqueous-phase hydrodeoxygenation of bio-derived phenols to cycloalkanes. *J. Catal.* **2011**, *280*, 8–16.
- (24) Sergeev, A. G.; Hartwig, J. F. Selective, nickel-catalyzed hydrogenolysis of aryl ethers. *Science* **2011**, *332*, 439–443.
- (25) Zhao, C.; Kou, Y.; Lemonidou, A. A.; Li, X. B.; Lercher, J. A. Hydrodeoxygenation of bio-derived phenols to hydrocarbons using RANEY Ni and Nafion/SiO₂ catalysts. *Chem. Commun.* **2010**, *46*, 412–414.
- (26) Echeandia, S.; Arias, P. L.; Barrio, V. L.; Pawelec, B.; Fierro, J. L. G. Synergy effect in the HDO of phenol over Ni–W catalysts supported on active carbon: Effect of tungsten precursors. *Appl. Catal., B* **2010**, *101*, 1–12.
- (27) Li, C. Z.; Zheng, M. Y.; Wang, A. Q.; Zhang, T. One-pot catalytic hydrocracking of raw woody biomass into chemicals over supported carbide catalysts: simultaneous conversion of cellulose, hemicellulose and lignin. *Energy Environ. Sci.* **2012**, *5*, 6383–6390.
- (28) Yan, N.; Yuan, Y.; Dykeman, R.; Kou, Y.; Dyson, P. J. Hydrodeoxygenation of lignin-derived phenols into alkanes by using nanoparticle catalysts combined with Brønsted acidic ionic liquids. *Angew. Chem., Int. Ed.* **2010**, *49*, 5549–5553.
- (29) Chen, J. Z.; Huang, J.; Chen, L. M.; Ma, L. L.; Wang, T. J.; Zakai, U. I. Hydrodeoxygenation of phenol and derivatives over an ionic liquid-like copolymer stabilized nanocatalyst in aqueous media. *ChemCatChem* **2013**, *5*, 1598–1605.
- (30) Furimsky, E. Catalytic hydrodeoxygenation. *Appl. Catal. A Gen.* **2000**, *199*, 147–190.
- (31) Hicks, J. C. Advances in C–O Bond transformations in lignin-derived compounds for biofuels production. *J. Phys. Chem. Lett.* **2011**, *2*, 2280–2287.
- (32) Chen, J. Z.; Wang, S. P.; Huang, J.; Chen, L. M.; Ma, L. L.; Huang, X. Conversion of cellulose and cellobiose into sorbitol catalyzed by Ruthenium supported on a polyoxometalate/Metal–Organic Framework hybrid. *ChemSusChem* **2013**, *6*, 1545–1555.

- (33) Vyver, S. V. D.; Geboers, J.; Schutyser, W.; Dusselier, M.; Eloy, P.; Dornez, E.; Seo, J. W.; Courtin, C. M.; Gaigneaux, E. M.; Jacobs, P. A.; Sels, B. F. Tuning the acid/metal balance of carbon nanofiber-supported nickel catalysts for hydrolytic hydrogenation of cellulose. *ChemSusChem* **2012**, *5*, 1549–1558.
- (34) Yan, N.; Zhao, C.; Dyson, P. J.; Wang, C.; Liu, L. T.; Kou, Y. Selective degradation of wood lignin over noble-metal catalysts in a two-step process. *ChemSusChem* **2008**, *1*, 626–629.
- (35) Yan, N.; Dyson, P. J. Transformation of biomass via the selective hydrogenolysis of C–O bonds by nanoscale metal catalysts. *Curr. Opin. Chem. Eng.* **2013**, *2*, 178–183.
- (36) Li, N.; Huber, G. W. Aqueous-phase hydrodeoxygenation of sorbitol with Pt/SiO₂–Al₂O₃: Identification of reaction intermediates. *J. Catal.* **2010**, *270*, 48–59.
- (37) Chao, K. J.; Chiou, B. H.; Cho, C. C.; Jeng, S. Y. Temperature-programmed desorption studies on ZSM-5 zeolites. *Zeolites* **1984**, *4*, 2–4.
- (38) Lobree, L. J.; Hwang, I. C.; Reimer, J. A.; Bell, A. T. Investigations of the state of Fe in H-ZSM-5. *J. Catal.* **1999**, *186*, 242–253.
- (39) Katada, N.; Igi, J.; Kim, M.; Niwa, J. Determination of the acidic properties of zeolite by theoretical analysis of temperature-programmed desorption of ammonia based on adsorption equilibrium. *J. Phys. Chem. B* **1997**, *101*, 5969–5977.
- (40) Cheng, K.; Kang, J. C.; Huang, S. W.; You, Z. Y.; Zhang, Q. H.; Ding, J. S.; Hua, W. Q.; Lou, Y. C.; Wang, Y. Mesoporous beta zeolite-supported Ruthenium nanoparticles for selective conversion of synthesis gas to C₅–C₁₁ isoparaffins. *ACS Catal.* **2012**, *2*, 441–449.
- (41) Chen, K. Y.; Tamura, M.; Yuan, Z. L.; Nakagawa, Y.; Tomishige, K. One-pot conversion of sugar and sugar polyols to *n*-alkanes without C–C dissociation over the Ir–ReO_x/SiO₂ Catalyst combined with H-ZSM-5. *ChemSusChem* **2013**, *6*, 613–621.
- (42) Furikado, I.; Miyazawa, T.; Koso, S.; Shimao, A.; Kunimori, K.; Tomishige, K. Catalytic performance of Rh/SiO₂ in glycerol reaction under hydrogen. *Green Chem.* **2007**, *9*, 582–588.
- (43) Hong, D. Y.; Miller, S. J.; Agrawal, P. K.; Jones, C. W. Hydrodeoxygenation and coupling of aqueous phenolics over bifunctional zeolite-supported metal catalysts. *Chem. Commun.* **2010**, *46*, 1038–1040.
- (44) Pepper, J. M.; Lee, Y. W. Lignin and related compounds. I. A comparative study of catalysts for lignin hydrogenolysis. *Can. J. Chem.* **1969**, *47*, 723–727.
- (45) Pepper, J. M.; Fleming, R. W. Lignin and related compounds. V. The hydrogenolysis of aspen wood lignin using rhodium-on-charcoal as catalyst. *Can. J. Chem.* **1978**, *56*, 896–898.
- (46) Ding, L. N.; Wang, A. Q.; Zheng, M. Y.; Zhang, T. Selective transformation of cellulose into sorbitol by using a bifunctional nickel phosphide catalyst. *ChemSusChem* **2010**, *3*, 818–821.
- (47) Yakovlev, V. A.; Khromova, S. A.; Sherstyuk, O. V.; Dundich, V. O.; Ermakov, D. Yu.; Novopashina, V. M.; Lebedev, M. Y.; Bulavchenko, O.; Parmon, V. N. Development of new catalytic systems for upgraded bio-fuels production from bio-crude-oil and biodiesel. *Catal. Today* **2009**, *144*, 362–366.
- (48) Zhu, X.; Mallinson, R. G.; Resasco, D. E. Role of transalkylation reactions in the conversion of anisole over HZSM-5. *Appl. Catal., A* **2010**, *379*, 172–181.
- (49) Wojciechowski, G.; Schroeder, G.; Zundel, G.; Brzezinski, B. Hydrogen bonds and hydrogen-bonded chains in complexes of 3-(Hydroxymethyl)-2,2'-biphenol with N-Bases FTIR and ¹H NMR Studies. *J. Phys. Chem. A* **2000**, *104*, 7469–7472.
- (50) Chen, J. Z.; Zhang, W.; Chen, L. M.; Ma, L. L.; Gao, H.; Wang, T. J. Direct Selective hydrogenation of phenol and derivatives over polyaniline-Functionalized Carbon Nanotube Supported Palladium. *ChemPlusChem* **2013**, *78*, 142–148.
- (51) Chen, A. B.; Zhao, G. Y.; Chen, J. Z.; Chen, L. M.; Yu, Y. F. Selective hydrogenation of phenol and derivatives over an ionic liquid-like copolymer stabilized palladium catalyst in aqueous media. *RSC Adv.* **2013**, *3*, 4171–4175.
- (52) Popov, A.; Kondratieva, E.; Goupil, J. M.; Mariey, L.; Bazin, P.; Gilson, J. P.; Travert, A.; Mauge, F. Bio-oils hydrodeoxygenation: adsorption of phenolic molecules on oxidic catalyst supports. *J. Phys. Chem. C* **2010**, *114*, 15661–15670.
- (53) Romero, Y.; Richard, F.; Renème, Y.; Brunet, S. Hydrodeoxygenation of benzofuran and its oxygenated derivatives (2,3-dihydrobenzofuran and 2-ethylphenol) over NiMoP/Al₂O₃ catalyst. *Appl. Catal. A Gen.* **2009**, *353*, 46–53.
- (54) Van Der Grift, C. J. G.; Wielers, A. F. H.; Jogh, B. P. J.; Van Beunum, J.; De Boer, M.; Versluijs-Helder, M.; Geus, J. W. Effect of the reduction treatment on the structure and reactivity of silica-supported copper particles. *J. Catal.* **1991**, *131*, 178–189.
- (55) Fan, G. Y.; Huang, W. J.; Wang, C. Y. In situ synthesis of Ru/RGO nanocomposites as a highly efficient catalyst for selective hydrogenation of halonitroaromatics. *Nanoscale* **2013**, *5*, 6819–6825.